Journal of Molecular Catalysis A: Chemical 304 (2009) 174–179

Contents lists available at ScienceDirect

Journal of Molecular Catalysis A: Chemical

journal homepage: www.elsevier.com/locate/molcata

A kinetic model for the oxidation of benzenethiol catalyzed by the $[Mo^{VI}O_2(O_2CC(S)(C_6H_5)_2)_2]^{2-}$ complex intercalated in a Zn(II)–Al(III) layered double hydroxide host

Antonio Ribera [a,*], Francisco Pérez-Pla [b,*], Elisa Llopis [b], Antonio Cervilla [b], Antonio Domenech [c]

[a] Instituto de Ciencia Molecular, Universidad de Valencia, Edificios Institutos de Paterna, Polígono La Coma s/n, E-46980 Paterna, Valencia, Spain
[b] Instituto de Ciencia de los Materiales, Universidad de Valencia, Edificios Institutos de Paterna, Polígono La Coma s/n, E-46980 Paterna, Valencia, Spain
[c] Departamento de Química Analítica, Universidad de Valencia, Dr. Moliner 50, E-46410 Burjassot, Valencia, Spain

ARTICLE INFO

Article history:
Received 28 July 2008
Received in revised form 30 January 2009
Accepted 6 February 2009
Available online 20 February 2009

Keywords:
Dioxomolybdenum
Molybdenum enzymes
CEPT reaction
Heterogeneous catalysis
Benzenethiol oxidation

ABSTRACT

The heterogeneous oxidation of benzenethiol catalyzed by the dianionic bis(2-sulfanyl-2,2-diphenylethanoxycarbonyl) dioxomolybdate (VI) complex intercalated into a Zn(II)–Al(III) layered double hydroxide (LDH) host have been investigated under aerobic conditions. The kinetics of the system has been analysed in detail. In ethanol, the benzenethiol is cleanly oxidized to diphenyl disulfide in the acidic media provided by the protonic resin Amberlite IR-120(H). The reaction is second-order in benzenethiol, and the apparent rate coefficient has been found to be proportional to the catalyst weight and inversely proportional to the initial concentration of the substrate. A catalytic cycle consistent with the kinetic data has been proposed. The catalytic cycle starts with the acid–base interaction of benzenethiol with the hydroxide anions present in the LDH to yield benzenethiolate anions which coordinate the Mo(VI) centres of the catalyst. The Mo(VI)-coordinated-sulphur species undergo decomposition to form neutral Mo(V) centres and benzenethiol radicals. In excess dioxygen, the Mo(V) species forms a peroxo-Mo centre which regenerates the Mo(VI) active sites by reacting with more benzenethiolate and protons, and producing hydroperoxyl radicals. The apparent activation energy is equal to 40 kJ mol^{-1}, which agrees with the reduction to Mo(V) of the sulphur-coordinate Mo(VI) centre as the rate limiting step.

The proposed catalytic cycle completes and generalizes the study of a reaction pathway previously reported, in which the bis(2-sulfanyl-2,2-diphenylethanoxycarbonyl) dioxomolybdate (VI) complex catalyzes the reduction of nitrobenzene to aniline coupled to the oxidation of benzenethiol to diphenyl disulfide under anaerobic conditions. The relevance of this catalyst-system lies in its ability to prevent the undesirable comproportionation reactions of the diverse oxidation state molybdenum intermediates making possible multiple-turnover oxidations of benzenethiol to diphenyl disulfide.

© 2009 Elsevier B.V. All rights reserved.

1. Introduction

Molybdenum is found in biological systems in a mononuclear form in the active site of a diverse group of enzymes that generally catalyze redox reactions [1–4]. Mononuclear molybdenum-containing enzymes are ubiquitous and participate in several biological processes occurring in nature, such as denitrification, the greenhouse effect, and pollution of the water soil.

The active site of these enzymes includes the metal atom coordinated to one or two pyranopterin molecules and to a variable number of ligands such as oxygen (oxo, hydroxo, water and aspartic acid) and sulphur (cysteines). With a few exceptions, these enzymes catalyze the transfer of an oxygen atom from water to the product (or vice versa) in reactions involving a net exchange of two electrons between the enzyme and substrate, and in which the metal ion cycles between the redox states IV and VI [5] with the paramagnetic Mo(V) state being an obligatory catalytic intermediate.

Modeling the active site of molybdoenzymes has been a topic of continuing research interest for the last decades, and a number of oxomolybdenum complexes have been synthesized providing insights into the biological mechanisms, and developing biomimetic reaction systems [5–9]. However, especially significant from the standpoint of the enzyme-catalyzed reaction would be the ability of these analogues to regenerate the active sites during the catalytic process. In the most cases, the oxidized and reduced forms of the molybdenum species react to form the corresponding oxo-bridged molybdenum (V) dimer according to the dinuclearization/comproportionation reaction (1).

$$Mo^{VI}O_2 + Mo^{IV}O \rightarrow OMo^{V}\text{–}O\text{–}Mo^{V}O \quad (1)$$

* Corresponding authors. Tel.: +34 963544419; fax: +34 963543273.
E-mail address: antonio.ribera@uv.es (A. Ribera).

1381-1169/$ – see front matter © 2009 Elsevier B.V. All rights reserved.
doi:10.1016/j.molcata.2009.02.009

In this way, systems capable to repress or eliminate the irreversible μ-oxo dimerization reaction (1) were synthesized in the early studies of molybdoenzymes [5], however most of them have the problem that are unstable in protic solvents. One of the strategies followed to solve this problem and mimic natural enzymes, by keeping apart from each other the oxidized and reduced molybdenum species just as proteins do in enzymes, was the encapsulation of coordination compounds in inorganic matrices like layered double hydroxides (LDHs) [10]. This strategy was later applied for the heterogenization of metal complexes in order to increase its stability and take advantage of the heterogeneous catalysis [11]. Even, the heterogenization has given the possibility to create bifunctional heterogeneous catalyst by combining a catalytically active transition metal centre with other groups present on the surface of the matrices [12].

Specifically, our synthetic approach to prevent dinuclearization and/or comproportionation reactions involves intercalation of an active oxomolybdenum complex into the interlamellar spaces of synthetic LDH system. Typically, cationic $Zn^{II}Al^{III}$ hydroxide sheets of composition $[Zn_{3-x}Al_x(OH)_6]^{x+}[NO_3]_x^- \cdot nH_2O$ that easily exchange nitrate by other anionic entities are used for this purpose. Whilst the intercalated anionic oxomolybdenum complex becomes freely accessible to the reactants, the "pillaring" complex itself is prevented from binuclear combination because of electrostatic interactions between it and the cationic layers that lead to its immobilization. This strategy turns the previously characterized $\{Mo^{VI}O_2[O_2CC(S)(C_6H_5)_2]_2\}^{2-}$ complex [13–15] into an heterogeneous system. The intercalated molybdenum complex anion has been shown by Mo-EXAFS [16] conjugated with other studies, to possess a trioxo group (in contrast to the dioxo unit that exists in the free complex), two Mo–S bonds, and one Mo–O bond. Thus, the intercalation between the hydroxide layers induces decoordination of both carboxylate groups and coordination of a single water molecule, so this supramolecular system should be better formulated as $[Zn_{3-x}Al_x(OH)_6]^{x+}[NO_3]_{x-y}^-\{Mo^{VI}O_3[O_2CC(S)(C_6H_5)_2]_2(H_2O)\}_{y/4}^{4-} \cdot nH_2O$, hereafter denoted by ZnAl-$[MoO_3(TBA)_2(H_2O)]$.

The purpose of this investigation is to elucidate the kinetics and mechanism of the heterogeneous oxidation by dioxygen of benzenethiol catalyzed by ZnAl-$[MoO_3(TBA)_2(H_2O)]$. First results of this investigation have been previously communicated [10,17,18], the present study being the aerobic pathway of the complete catalytic cycle developed by this molybdoenzyme analogue intercalated into a LDH system. The anaerobic pathway, with nitrobenzene as the oxidant, was already presented [19,20] being aniline the only product detected through a reaction that consumes benzenethiol. This previous study exposed a well-defined catalytic cycle with multiple-turnovers reductions of nitrobenzene to aniline without appreciable deactivation of the catalyst.

2. Experimental

2.1. Materials

All chemicals utilized: benzenethiol, nitrobenzene, and ethanol were analytical grade and used as received from Fluka. The Amberlite IR-120(H) was provided by Sigma–Aldrich. The catalyst was prepared following a previously described method [17].

2.2. Kinetic runs

The heterogeneous catalytic activity of ZnAl-$[MoO_3(TBA)_2(H_2O)]$ for the oxidation of benzenethiol (PhSH) was investigated under dioxygen. Reactions were carried out in a 50-mL flask equipped with a condenser, a line on the top to flow the oxygen gas and a trap filled with silicon at the end for closing the system. In a typical experiment, a constant amount of ZnAl-$[MoO_3(TBA)_2(H_2O)]$ (250 mg, 0.084 mmol of molybdenum complex) and 250 mg of solid Amberlite IR-120(H) were added to a solution containing a variable concentration of PhSH (ranged from 1 to 9 mol dm^{-3}, with a total volume of 35 cm^3) in ethanol under oxygen atmosphere (1 atm), and vigorously stirred to ensure a rapid admission of dioxygen into the liquid phase. Aliquots of 100 μL were taken out, cooled, filtered to remove the catalyst (using a glass/Teflon syringe and a special filter for very small volume with a diameter of 4 mm in which the retained volume is less than 7.5 μL adapted to the syringe through a Luer system). After stopping the reaction, 1 μL of an internal standard (nitrobenzene) was added and, finally, 0.5 μL of these solutions were injected into a gas chromatograph (GC). Gas chromatography–mass spectrometry (GC–MS) was used to identify the products formed in the reactions. The kinetic runs were followed at least for a period of 4 days.

2.3. Gas chromatography analyses

Gas chromatography analyses were performed on a Varian Star 3300 chromatograph, working in split mode (split ratio 1:50), equipped with a FID detector and a DB-5 column (30 m × 0.32 mm, film thickness = 0.25 μm). Mass spectrometry data were obtained on a Fisons MD 800 mass spectrometer coupled to a DB-5 column (60 m × 0.32 mm, film thickness = 0.25 μm).

The experimental conditions used for GC and GC–MS were as follows. The oven was heated to 50 °C during 5 min; then the temperature was raised from 50 °C to 140 °C at 15 °C/min, and from 140 °C to 300 °C at 35 °C/min. During the analyses, both the injector and detector were maintained at 300 °C for 1 min. Under such conditions the retention time obtained for reactants and products were: ethanol 1.6 min, benzenethiol 8.1 min, nitrobenzene 10.2 min, and diphenyl disulfide 15.6 min. Concentration at various times were determined by signal integration. Retention times of products agreed with those of authentic samples.

3. Results and discussion

Carefully monitored GC–MS experiments showed that diphenyl disulfide, Ph_2S_2, is the only product formed from the PhSH oxidation, using ZnAl-$[MoO_3(TBA)_2(H_2O)]$ as catalyst and dioxygen as the oxidizing agent. Under oxygen atmosphere, the internal standard, $PhNO_2$, remained unaltered.

3.1. Catalyst activity

The catalyst activity was estimated as the turnover frequency at zero time. This quantity was calculated by dividing the initial rate for the benzenethiol conversion by the number of molybdenum complex mol obtained by atomic absorption analysis of molybdenum. The catalyst exhibits a moderate activity as the measured turnover frequency ranges between 10^{-6} and 3.2×10^{-5} s^{-1} (see Table 1).

Turnover frequencies increase as temperature increases, as expected. However, it is remarkable the decrease in the turnover frequency as the initial concentration of benzenethiol increases.

3.2. The rate law

The catalytic activity of ZnAl-$[MoO_3(TBA)_2(H_2O)]$ has been tested by carrying out the three series of reactions presented in Table 2. In each series, the initial concentration of benzenethiol was varied among kinetic runs, keeping constant the oxygen pressure, the catalyst, and Amberlite concentrations. Only the temperature was varied among the series.

Table 1
Turnover frequency as a function of temperature and initial concentration of benzenethiol.

T (K)	$[PhSH]_{t=0}$ (mol dm^{-3})	r_0 ($\times 10^7$ mol s^{-1})	Turnovers ($\times 10^3$ s^{-1})
313.2 ± 0.2	1.410 ± 0.001	0.82	0.97
	2.805	1.70	2.01
	7.313	2.52	2.99
	9.294	2.68	3.18
333.22 ± 0.2	1.411	1.97	2.33
	3.048	4.57	5.42
	4.908	9.00	10.6
	5.647	11.18	13.2
	6.816	13.90	16.5
353.2 ± 0.2	0.989	3.58	4.25
	1.418	5.03	5.98
	2.433	8.32	9.88
	3.897	14.88	17.6
	4.761	19.03	22.6
	6.871	27.03	32.1

After completion of the kinetic runs, the solutions were subjected to Millipore filtration and their molybdenum content was determined by atomic absorption. Analysis of both solution and catalyst did not indicate leaching of the molybdenum complex.

In all runs, the benzenethiol concentration decreased with time under constant pressure of dioxygen; the mathematical analysis of concentration–time curves indicate that all of them are second-order with regard to the benzenethiol, as shown in Fig. 1; the analysis of variance of the residuals assessed, by means of the correlation coefficients and Fisher F-tests [21], that second-order was preferred 14 times over the 15 runs carried out. Thus, kinetic data were fitted to Eq. (2), where k_{app} is an apparent second-order rate coefficient. The values for k_{app} are collected in Table 2.

$$\frac{1}{\alpha} - 1 = k_{app}[PhSH]_{t=0}t, \quad \alpha = \frac{[PhSH]}{[PhSH]_{t=0}} \tag{2}$$

The influence of the catalyst concentration on the rate of the overall oxidation process was tested by carrying out blank-reactions in which the catalyst was substituted by its LDH host; blanks were carried out in the same experimental conditions of temperature and concentration than those of the series at 353.2 K. Table 3 shows the relative conversion degree of benzenethiol into disulfide after 7 h, and Fig. 2A presents a typical reaction-time profile for both the catalyzed and uncatalyzed reaction.

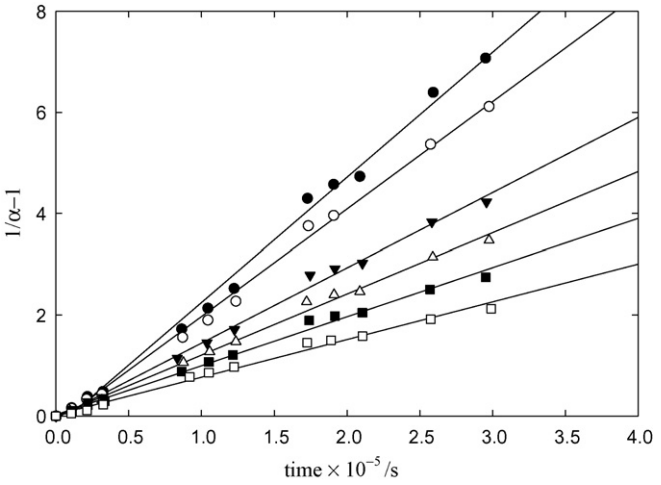

Fig. 1. Second-order plot for the oxidation of benzenethiol in ethanol at 353.15 K under dioxygen at 1 atm. Added 250 mg of solid Amberlite IR-120(H) and 250 mg of ZnAl-$[MoO_3(TBA)_2(H_2O)]$. $\alpha = [PhSH]/[PhSH]_{t=0}$, $[PhSH]_{t=0}$ in mol dm^{-3}: (●) 0.989, (○) 1.418, (▼) 2.433, (▽) 3.897, (■) 4.761 and (□) 6.871. The rate constants are collected in Table 2.

Table 3
Relative conversion degree of benzenethiol into disulfide for the catalyzed (†) and uncatalyzed (††) oxidation.

n_0 (PhSH) (mol)	$\lvert(n_0 - n_t)/n_0 \times 10^2\rvert^{\dagger}$	$\lvert(n_0 - n_t)/n_0 \times 10^2\rvert^{\dagger\dagger}$
0.027	86.5	6.6
0.040	84.3	4.0
0.080	79.3	1.9
0.16	75.8	2.4
0.23	71.5	2.1
0.58	65.7	5.0

n_0 = initial number of benzenethiol moles; n_t = number of benzenethiol moles remaining after 25×10^3 s (7 h) of reaction.

The uncatalyzed reaction stops suddenly after an initial decrease of 2–6% of the benzenethiol concentration, this quantity remaining constant after 4 days of reaction, whilst the catalyzed system reaches 70–85% of relative conversion degree of benzenethiol into disulfide by this time. There is little doubt, therefore, that reaction is almost entirely proceeding among the catalyst layers, and thus, the homogeneous benzenethiol auto-oxidation is efficiently repressed by the acidic media provided by the Amberlite protonic resin.

Table 2
Second-order kinetic coefficients[a] for the benzenethiol oxidation as a function of temperature and initial benzenethiol concentration.

T (K)	$[PhSH]_{t=0}$ (mol dm^{-3})	k_{app} ($\times 10^6$ s^{-1} mol^{-1} dm^3)	R^b	F^b	R^c	F^c
313.2 ± 0.2	1.410 ± 0.001	2.19 ± 0.03	0.998	7893	0.98	492
	2.805	0.901 ± 0.014	0.998	3345	0.98	546
	7.313	0.319 ± 0.014	0.98	469	0.993	1763
	9.294	0.186 ± 0.024	0.998	5603	0.998	1684
333.22 ± 0.2	1.411	3.60 ± 0.04	0.998	5167	0.98	382
	3.048	1.34 ± 0.02	0.997	3390	0.98	389
	4.908	0.69 ± 0.01	0.996	2467	0.98	399
	5.647	0.559 ± 0.008	0.997	3740	0.98	537
	6.816	0.304 ± 0.005	0.997	3487	0.98	567
353.2 ± 0.2	0.989	23.4 ± 0.7	0.997	938	0.97	170
	1.418	13.9 ± 0.4	0.993	624	0.97	167
	2.433	6.1 ± 0.1	0.998	2323	0.97	187
	3.897	3.13 ± 0.05	0.998	2423	0.97	185
	4.761	2.08 ± 0.04	0.997	1414	0.97	190
	6.871	1.12 ± 0.03	0.995	910	0.97	176

[a] Solvent ethanol containing 250 mg of Amberlite IR-120(H) and 250 mg of catalyst; reaction carried out under dioxygen at 1 atm.
[b] Correlation coefficient (R) and F-test obtained by fitting experimental data to a second-order model.
[c] Correlation coefficient (R) and F-test obtained by fitting experimental data to a first-order model.

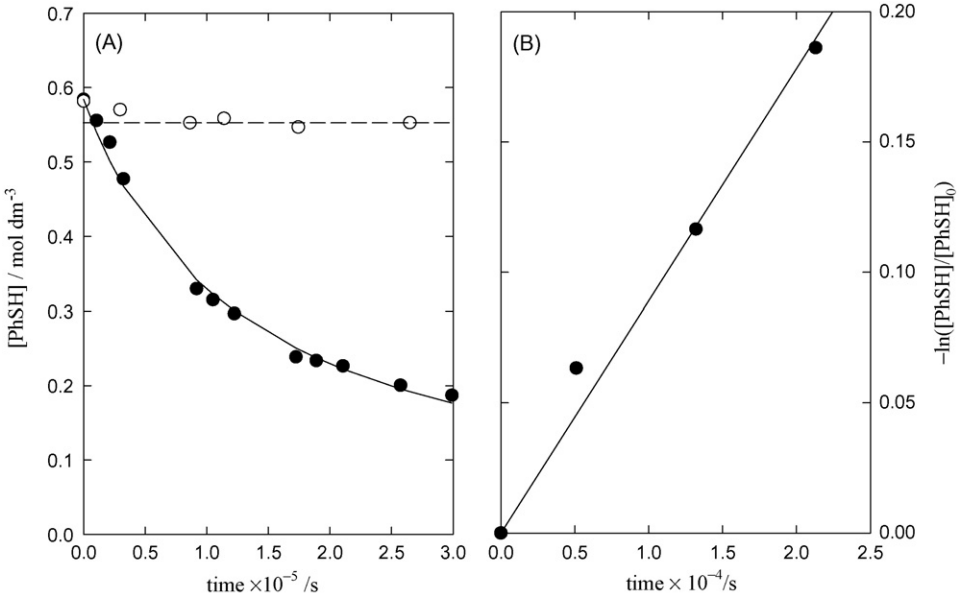

Fig. 2. Influence of the proton source over the oxidation of benzenethiol. (A) In presence of Amberlite IR-120(H): kinetic behavior of the catalyzed (●) and uncatalyzed (○) benzenethiol oxidation in ethanol in the presence of 250 mg of Amberlite IR-120(H) at 353.15 K. Catalyzed reaction (added 250 mg of ZnAl-[$MoO_3(TBA)_2(H_2O)$]) and uncatalyzed reaction (added 250 mg of the LDH host). Both reaction systems contained initially 6.87 mol dm^{-3} of benzenethiol. (B) Using water as proton source: plot showing the first-order kinetic behavior of the homogeneous auto-oxidation of a solution of benzenethiol (0.52 g) in ethanol (14.03 g) containing 253 mg of the LDH host and water (6.10 g) as the proton source.

This conclusion is corroborated by the kinetic experiment shown in Fig. 2B in which the catalyst has been replaced by its LDH host and the Amberlite has been substituted by water as the proton source. Under such conditions, the acid–base equilibrium in homogeneous phase (3) is reached,

$$PhSH + B \leftrightarrow PhS^- + BH^+ \qquad (B = H_2O, OH^-) \tag{3}$$

and the benzenethiolate ions formed react with dioxygen in the liquid phase. It is worth noting, that the described homogeneous reaction obeys a first-order kinetics, as observed in other homogeneous thiol auto-oxidations by dioxygen [22,23], whilst the molybdenum-catalyzed reaction is second-order with regard to the benzenethiol indicating that both reactions proceed through different mechanisms.

The k_{app} values were found to be dependent upon the initial concentration of benzenethiol. It was observed the higher the initial concentration of benzenethiol, the lower was the value of k_{app} (Table 2). The best expression fitting the experimental data was Eq. (4) (see Fig. 3):

$$\ln(k_{app}) = \ln(k) - a\ \ln([PhSH]_0) \tag{4}$$

Eq. (4) will be explained latter in terms of the acid–base equilibrium suffered by the benzenethiol inside the hydroxide sheets. The k and a parameters measured for each series are collected in Table 4.

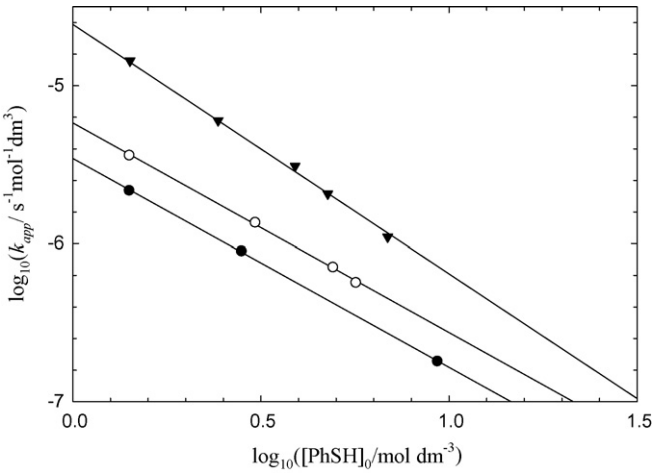

Fig. 3. Dependence of the second-order kinetic coefficient on the temperature and the initial concentration of benzenethiol: (▼) 353.15 K, (○) 333.15 K and (●) 313.15 K.

3.3. The mechanism of reaction

The mechanism shown in Scheme 1 was proposed to endow with chemical meaning the empirical rate coefficients. The mechanism generalizes the previous one reported for the reduction of nitrobenzene to aniline catalyzed by the complex occurring under anaerobic conditions [24].

Table 4
Dependence of parameters k and a from Eq. [3] on temperature. Apparent activation parameters for the benzenethiol oxidation.

$\ln(k_{app}) = \ln(k) - a\ln([PhSH]_0)$ [4]			
T (K)	k ($\times 10^6$ s^{-1} M)	a	R
313.2 ± 0.2	3.4 ± 0.2	1.28 ± 0.04	0.99
333.2	5.7 ± 0.1	1.33 ± 0.02	0.999
353.2	24.0 ± 0.1	1.55 ± 0.04	0.999
$\Delta H^{\neq}$ (kJ mol^{-1})	44 ± 12	$\Delta S^{\neq}$ (J K^{-1} mol^{-1})	−200 ± 40

The apparent activation parameters were obtained by fitting k values to the Eyring equation: $\ln(k/T) = (\ln(k_B/h) + \Delta S^{\neq}/R) - \Delta H^{\neq}/(RT)$.

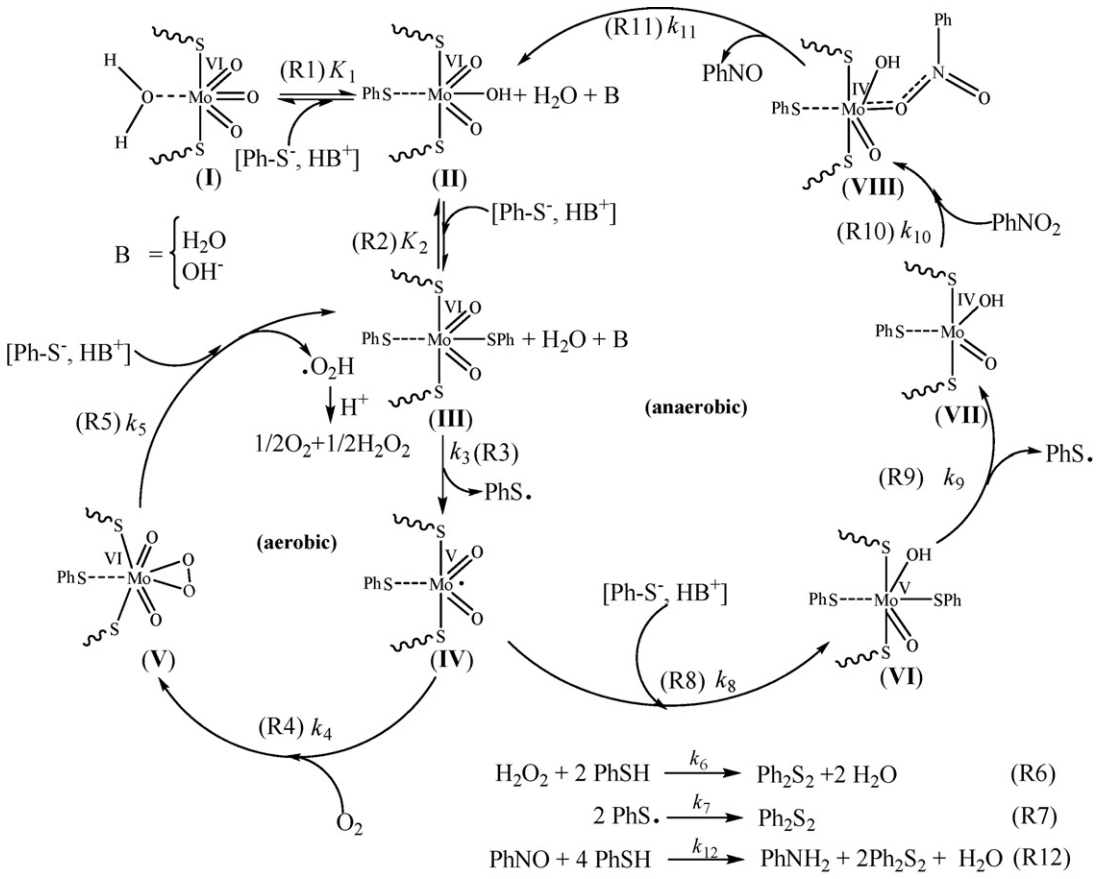

Scheme 1.

The mechanism essentially consists of two coupled cycles, one of them working under anaerobic conditions, and responsible for the nitrobenzene reduction, and a second cycle (aerobic) whose main effect is the oxidation of benzenethiol to diphenyl disulfide and the production of hydrogen peroxide and water.

The aerobic cycle starts with the acid–base equilibrium (3) occurring between the water (or OH^-) present on the catalyst layers and benzenethiol. The formed benzenethiolate ion-pairs react with the Mo^{VI} active centres (**I**) yielding the activated Mo^{VI} species (**II** and **III**), all of them in equilibrium with the benzenethiolate anions. This kind of sulphur coordination for Mo^{VI} has been proposed for reaction mechanisms involving enzymatic reducing molybdoenzymes [19] and for the homogeneous oxidation of benzenethiol to diphenyl disulfide by $[Bu_4N]_2[Mo^{VI}O_2(mnt)_2]$ (mnt = 1,2-dicyano-ethylene-dithiolate) [24].

Species (**III**) undergo homolytic break of the Mo–S bond to form Mo^V neutral species (**IV**) and benzenethiol radicals; the existence of Mo^V species are in agreement with the presence of dimeric Mo^V complexes observed during the homogeneous aerobic oxidation of thiols [14]. These dimers are precisely who prevent the subsequent reduction of Mo^V to Mo^{IV} in solution breaking the catalytic cycle.

Now, species (**IV**) react following different paths depending upon the presence of dioxygen in the media. If dioxygen is present, species (**IV**) will add dioxygen to form a peroxo-Mo-complex (**V**) able to react with more benzenethiolate closing the aerobic cycle, and yielding the Mo^{VI} species (**III**) and hydroperoxyl radicals which disproportionate in protic media. The anaerobic cycle starts with species (**IV**) coordinating to a new benzenethiolate ion-pair to form species (**VI**) which undergo decomposition yielding the Mo^{IV} species (**VII**) and benzenethiol radical. Now, the cycle closes due to Mo^{IV} oxidizes to Mo^{VI} via a direct oxygen atom cession from a nitrobenzene molecule.

In a previous work [19,20], we demonstrated that reduction of Mo^V to Mo^{IV} was rate limiting for the nitrobenzene reduction under anaerobic conditions. The experimental results obtained in this work confirm our previous results since nitrobenzene is not reduced to aniline in excess dioxygen, indicating that Mo^V species are reacting faster with dioxygen than with benzenethiolate ion-pairs to yield species (**VI**).

The rate law deduced from the mechanism depicted in Scheme 1 is given by Eq. (5) (see supplementary material):

$$\frac{d[Ph_2S_2]}{dt} = \frac{1}{2}\frac{k_3K_1K_2[Mo]}{1 + K_1(1 + (k_3/k_5)K_2)[PhS^-] + (k_3/k_4)K_1K_2([PhS^-]^2/[O_2])}[PhS^-]^2 \quad (5)$$

The rate law (5) is simplified assuming the benzenethiolate ion-pair is at low concentration due to PhSH is a weak acid and water, the proton acceptor, is also present at low concentration on the catalyst layers. Under such conditions, Eq. (5) simplifies to Eq. (6) (see supplementary material), where $[PhSH]_T$ stands for the total benzenethiol concentration ($[PhSH]_T = [PhSH] + [PhS^-]$), B for that of the free base (water, OH^-), and K_a is the equilibrium constant relating the concentrations of free base, ion-pair benzenethiolate, and benzenethiol:

$$-\frac{d[PhSH]_T}{dt} \approx k_3K_1K_2K_a^2[Mo][B]^2[PhSH]_T^2 \quad (6)$$

Eq. (6) is second-order with regard the benzenethiol as observed in kinetic runs, and allows understanding the observed decrease on the turnover frequency as the initial benzenethiol concentration increases (see Table 2). In fact, the empirical rate coefficient in Eq. (4) is interpreted as Eq. (7) after comparison to Eq. (6). It is worth noting that Eq. (7) is not depending apparently upon the

initial benzenethiol concentration:

$$k_{app} \approx k_3 K_1 K_2 K_a^2 [Mo][B]^2 \quad (7)$$

However, the total amount of free base ([B]) is determined by the initial concentration of benzenethiol ($[PhSH]_0$). The (PhS^-, HB^+) ion-pair concentration is almost equal to the initial amount of water on the layers ($[B]_0$) due to the amount of water (and OH^-) on the catalyst layers is small compared to that of benzenethiol. Under these conditions, Eq. (8) applies:

$$[B] \approx \frac{1}{K_a} \frac{[B]_0}{[PhSH]_0} \quad (8)$$

After substitution of Eq. (8) into Eq. (7) and taking logarithms, Eq. (9) is obtained:

$$\log(k_{app}) \approx \log(k_3 K_1 K_2 [Mo][B]_0^2) - 2\ \log([PhSH]_0) \quad (9)$$

Eq. (9) agrees qualitatively with the empirical Eq. (4), endowing with chemical sense the empirical coefficients k and a as follows:

$$k \approx k_3 K_1 K_2 [Mo][B]_0^2, \quad a \approx 2 \quad (10)$$

Nevertheless, the value found for the a parameter ranges from 1.3 to 1.6 probably due to the activity of water among the catalyst layers must be considered instead of its concentration.

3.4. Activation parameters

The apparent activation parameters calculated from the Eyring's plot are collected in Table 4. There is two possible rate limiting steps for the aerobic cycle, the reduction of Mo(VI) species (**III**) to form the Mo(V) centres (**I**) as well the re-oxidation of such species to Mo(VI) by dioxygen. The apparent activation enthalpy (40 kJ mol^{-1}) agrees with a limiting step consisting of the reduction of Mo^{VI} centre to Mo^{V} (R3). Similar activation energies have been observed for the catalytic oxidation of benzenethiol to diphenyl disulfide by transition metal ions in which the monoelectronic electron transfer toward the central cation is rate limiting [25].

On the other hand, the previously reported enthalpy of activation for the anaerobic cycle (77 kJ mol^{-1}) is in agreement with the overall rate limiting step being the Mo^{V} reduction to Mo^{IV} (reactions (R8) and (R9) in Scheme 1). Comparison of both activation energies allow concluding that the aerobic cycle, which involves a change in the oxidation state from VI to V, is favored energetically with regard to the anaerobic one, which involves changes in the oxidation state from V to IV at the rate limiting step. This fact correlates with the observation that aniline is produced from nitrobenzene only when the system works at high benzenethiol concentration or in absence of dioxygen.

4. Concluding remarks

In conclusion, the present investigation together with the previously reported, demonstrates that the intercalation of the bis(2-sulfanyl-2,2-diphenylethanoxycarbonyl) dioxomolybdate (VI) complex into a Zn(II)–Al(III) layered double hydroxide host is a suitable strategy to prepare molybdenum redox catalysts in which the dinuclearization and/or comproportionation reactions of the IV and VI oxidation states is prevented. The resulting catalyst is able to reduce nitrobenzene to aniline in a closed anaerobic cycle as well to oxidize benzenethiol to diphenyl disulfide in an alternative cycle working under aerobic conditions. Specifically, the prepared catalyst is able to oxidize efficiently benzenethiol by oxygen even in the acidic media provided by protonic resins, in which the homogeneous reaction is almost inhibited, due to the presence of additional basic centre in the hydroxide sheets, which carry out the benzenethiolate activation. This fact together with the redox properties of the molybdenum centres, endows the catalyst of a bifunctionality able to change stepwise its oxidation state from **IV** to **VI**, allow explaining the observed features through the reaction set summarized in the catalytic cycles appearing in Scheme 1.

Acknowledgments

Financial support from the Spanish Ministerio de Ciencia e Innovación (Project CTQ-2005-09385) and Generalitat Valenciana are gratefully acknowledged. A.R. thanks the Spanish Government for a Ramón y Cajal contract.

Appendix A. Supplementary data

Supplementary data associated with this article can be found, in the online version, at doi:10.1016/j.molcata.2009.02.009.

References

[1] A. Sigel, H. Sigel, Molybdenum and Tungsten: Their Roles in Biological Processes, Metal Ions in Biological Systems, vol. 39, Marcel Dekker, New York, 2002.
[2] R. Hille, Chem. Rev. 96 (1996) 2757–2816.
[3] R. Hille, Trends Biochem. Sci. 27 (2002) 360–367.
[4] E.I. Stiefel, D. Coucouvanis, W.E. Newton, Molybdenum Enzymes, Cofactors, and Model Systems, ACS Symposium Series 535, Washington, DC, 1992.
[5] J.H. Enemark, J.A. Cooney, J.J. Wang, R.H. Holm, Chem. Rev. 104 (2004) 1175–1200.
[6] J.J. Wang, C. Tessier, R.H. Holm, Inorg. Chem. 45 (2006) 2979–2988.
[7] J.H. Enemark, A.V. Astashkin, A.M. Raitsimring, Dalton Trans. (2006) 3501–3514.
[8] J.J. Wang, S. Groysman, S.C. Lee, R.H. Holm, J. Am. Chem. Soc. 129 (2007) 7512–7513.
[9] S. Groysman, R.H. Holm, Inorg. Chem. 46 (2007) 4090–4102.
[10] A. Cervilla, A. Corma, V. Fornés, E. Llopis, P. Palanca, F. Rey, A. Ribera, J. Am. Chem. Soc. 116 (1994) 1595–1596.
[11] A. Fuerte, M. Iglesias, F. Sanchez, A. Corma, J. Mol. Catal. A 211 (2004) 227–235.
[12] V.N. Nemykin, A.E. Polshyna, S.A. Borisenkova, V.V. Strelko, J. Mol. Catal. A 264 (2007) 103–109.
[13] P. Palanca, T. Picher, V. Sanz, P. Gomez-Romero, E. Llopis, A. Domenech, A. Cervilla, J. Chem. Soc., Chem. Commun. (1990) 531–533.
[14] V. Sanz, T. Picher, P. Palanca, E. Llopis, J.A. Ramirez, D. Beltran, A. Cervilla, Inorg. Chem. 30 (1991) 3113–3115.
[15] E. Llopis, A. Domenech, J.A. Ramirez, A. Cervilla, P. Palanca, T. Picher, V. Sanz, Inorg. Chim. Acta 189 (1991) 29–34.
[16] A. Corma, F. Rey, J.M. Thomas, G. Sankar, G.N. Greaves, A. Cervilla, E. Llopis, A. Ribera, Chem. Commun. (1996) 1613–1614.
[17] A. Cervilla, E. Llopis, A. Ribera, A. Corma, V. Fornés, F. Rey, J. Chem. Soc., Dalton Trans. (1994) 2953–2957.
[18] A. Corma, V. Fornés, F. Rey, A. Cervilla, E. Llopis, A. Ribera, J. Catal. 152 (1995) 237–242.
[19] A. Cervilla, F. Pérez-Pla, A. Ribera, E. Llopis, A. Doménech, Int. J. Chem. Kinet. 33 (2001) 212–224.
[20] A. Cervilla, A. Corma, V. Fornés, E. Llopis, F. Pérez, F. Rey, A. Ribera, J. Am. Chem. Soc. 117 (1995) 6781–6782.
[21] P. Gans, Data Analysis in the Chemical Sciences, Wiley, Chichester, 1992.
[22] T.J. Wallace, A. Schriesheim, W. Bartok, J. Org. Chem. 28 (1963) 1311–1314.
[23] T.J. Wallace, A. Schriesheim, J. Org. Chem. 27 (1962) 1514–1516.
[24] P.K. Chaudhury, K. Narajan, A. Kumar, R. Maiti, S.K. Das, S. Sarkar, Ind. J. Chem. 42A (2003) 2223–2227.
[25] G.A. Bagiyan, I.K. Koroleva, N.V. Soroka, A.V. Ufimtsev, Russ. Chem. Bull. Int. Ed. 52 (2003) 1135–1141.